Molecular engineering of benzenesulfonyl analogs for visual hydrogen polysulfide fluorescent probes based on Nile red skeleton

Qian Feng, Yiming Song, Yixuan Ma, Yan Deng, Pengyue Xu, Kangjia Sheng, Yongmin Zhang, Jianli Li, Shaoping Wu

Molecular engineering of benzenesulfonyl analogs for visual hydrogen polysulfide fluorescent probes based on Nile red skeleton

Qian Feng[a,§], Yiming Song[b,§,*], Yixuan Ma[a], Yan Deng[a], Pengyue Xu[a], Kangjia Sheng[a], Yongmin Zhang[c], Jianli Li[d], Shaoping Wu[a,*]

[a] Key Laboratory of Resource Biology and Biotechnology in Western China, Ministry of Education, Biomedicine Key Laboratory of Shaanxi Province, Northwest University, Xi'an, 710069, P. R. China.

[b] School of Chemical Engineering, Northwest University, 229 Taibai Road, Xi'an, Shaanxi, 710069, P. R. China.

[c] Sorbonne Université, CNRS, Institut Parisien de Chimie Moléculaire, UMR 8232, 4 place Jussieu, 75005 Paris, France.

[d] Key Laboratory of Synthetic and Natural Functional Molecule Chemistry of Ministry of Education, College of Chemistry & Materials Science, Northwest University, Xi'an, Shaanxi, 710127, P. R. China.

[§] These authors contributed equally to this work.

[*] Corresponding author: *ymsong@nwu.edu.cn, wushaoping@nwu.edu.cn*

Abstract: Hydrogen polysulfide (H_2S_n, n>1) has a valuable function in various aspects of biological regulation. Therefore, it is of great significance to realize the visual monitoring of H_2S_n levels in vivo. Herein, a series of fluorescent probes **NR-BS** were constructed by changing types and positions of substituents on the benzene ring of benzenesulfonyl. Among them, probe **NR-BS4** was optimized due to its wide linear range (0~350 μM) and little interference from biothiols. In addition, **NR-BS4** has a broad pH tolerance range (pH = 4~10) and high sensitivity (0.140 μM). In addition, the PET mechanism of probe **NR-BS4** and H_2S_n was demonstrated by DFT calculations and LC-MS. The intracellular imaging studies indicate that **NR-BS4** can be successfully devoted to monitor the levels of exogenous and endogenous H_2S_n *in vivo*.

Keywords: Nile red; Fluorescent probe; H_2S_n; Cell imaging; Zebrafish imaging

1. Introduction

Reactive sulfur species (RSS) have redox activity under physiological conditions, mainly including reduced glutathione (GSH), sulfur dioxide (SO_2), cysteine (Cys), sulfite/bisulfite (SO_3^{2-}/HSO_3^-), homocysteine (Hcy), hydrogen polysulfide (H_2S_n, n>1) and hydrogen sulfide (H_2S). RSS give full play to superiority in adjusting redox activity [1] and maintaining mitochondrial health [2]. However, RSS disorders can also induce a variety of diseases such as arteriosclerosis [3], diabetes [4], neurodegenerative diseases [5], aging [6] and schizophrenia [7]. Among these RSS molecules, H_2S is the third gas signal molecule with biological activity after NO and CO, which has been extensively studied in recent years [8-11]. With further research, H_2S_n (n>1) has been found to be more effective than H_2S in adjusting the activities of ion channels, transcription factors, protein kinases and tumor suppressors [12,13]. Obviously, many of the biological functions previously thought to be attributed to H_2S may actually be performed by H_2S_n [14]. Moreover, H_2S_n has many biological functions such as anti-oxidation ion channel activation and nephrotoxicity inhibition [15-17]. In order to have a deeper understanding of its formation, molecular reactions and regulatory mechanisms, it is necessary to exploit accurate and highly specific tools to monitor H_2S_n level in vivo.

Although the traditional monitoring technologies mainly involving ultraviolet-visible spectroscopy [18], mass spectrometry [19] and high-performance liquid chromatography [20] could detect H_2S_n in trace amounts, they usually require complex sample pretreatment, and the most critical problem is that they cannot be monitored in real time in organisms. At present, fluorescence analysis technology has become the most feasible method for detecting H_2S_n due to its highly temporal and spatial resolution, high sensitivity, non-invasive and fast real-time imaging [21,22]. The first H_2S_n-specific probe, **DSP**, was reported by Xian's group in 2014 [23], and a great quantity of H_2S_n fluorescent sensors have been ensued, primarily including 2-fluoro-5-nitrobenzoic ester [24], aziridine [25], nitro [26], cinnamate ester [27], acrylate ester [28] and 2-benzoylsulfanylbenzoic acid [21] as recognition groups **(**Fig.

1). However, these probes have certain limitations, such as poor selectivity, long response time, and narrow linear range. Therefore, new recognition units need to be proposed for the development of H_2S_n probes.

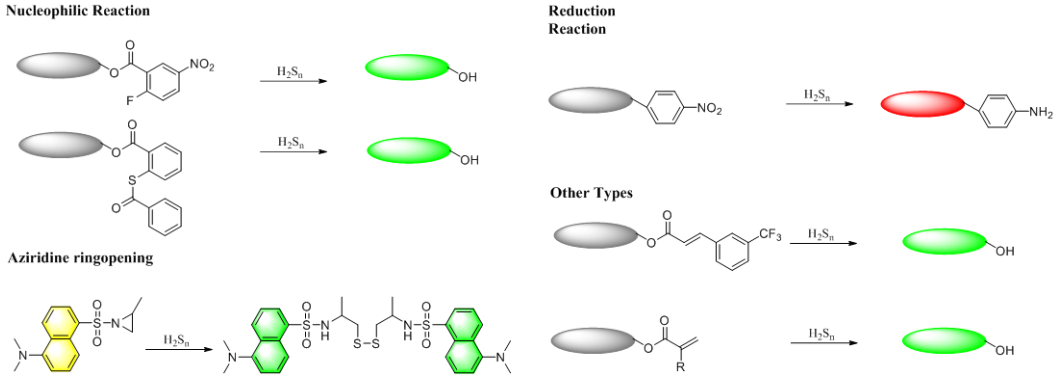

Fig. 1. Commonly used recognition sites for H_2S_n probes.

Based on the fact that 2, 4-dinitrobenzenesulfonyl is a classical recognition site for biothiols and the strong nucleophilicity of H_2S_n compared to biothiols, we envisioned an engineering to explore between different benzenesulfonyl analogs and efficient H_2S_n fluorescent probes (Fig. **2**). To this end, a series of fluorescent probes **NR-BS** based on Nile red skeleton were designed and synthesized. Among them, **NR-BS4** with 3-hydroxy NR as the skeleton and 2-nitrobenzenesulfonyl as the reaction site has the advantages of wide linear range (0~350 μM) and high selectivity. Most importantly, probe **NR-BS4** has low toxicity and superior ability to detect H_2S_n level in cells and zebrafish.

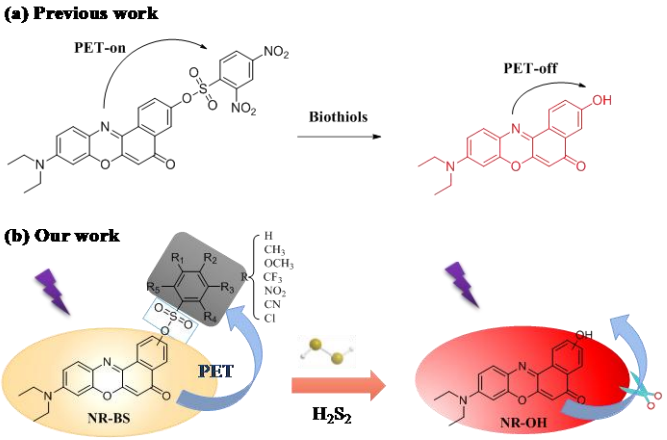

Fig. 2. Design of novel probes **NR-BS**.

2. Experimental section

2.1. Synthesis of probe **NR-BS4**

Compound **2b** (33.4 mg, 0.100 mmol, 1.00 equiv.) was dissolved in DCM and cooled to 0℃. Et_3N (55.0 μL, 0.210 mmol, 2.10 equiv.), 2-nitrobenzene sulfonyl chloride (44.3 mg, 0.200 mmol, 2.00 equiv.) were dissolved in the main reaction flask and allowed to react for 2 h at room temperature. After monitoring by TLC to ensure that compound **2b** was exhausted, the reaction mixture was extracted with DCM and water, the DCM layer was dried and evaporated. Then, the residue was purified by flash column chromatography (DCM:MeOH = 200:1) to give **NR-BS4** (89.2% yield). ^{1}H NMR (400 MHz, C_5D_5N) δ 8.52 (s, 1H), 8.17 (d, J = 7.9 Hz, 1H), 8.07 (d, J = 8.0 Hz, 1H), 7.86 - 7.69 (m, 3H), 7.65 (d, J = 7.7 Hz, 2H), 6.76 (d, J = 8.9 Hz, 1H), 6.58 (d, J = 1.4 Hz, 2H), 3.36 (t, J = 16.7 Hz, 4H), 1.10 (t, J = 7.0 Hz, 6H); ^{13}C NMR (101 MHz, C_5D_5N) δ 181.46, 152.63, 151.64, 147.15, 137.82, 136.53, 134.48, 132.70, 132.38, 131.66, 130.97, 128.36, 127.71, 125.65, 125.59, 125.14, 117.28, 112.37, 110.56, 105.21, 104.17, 96.45, 44.97, 12.39. HRMS ($C_{26}H_{21}N_3O_7S$): calcd. For $[M+H]^+$ 520.1178; found: $[M+H]^+$ 520.1071.

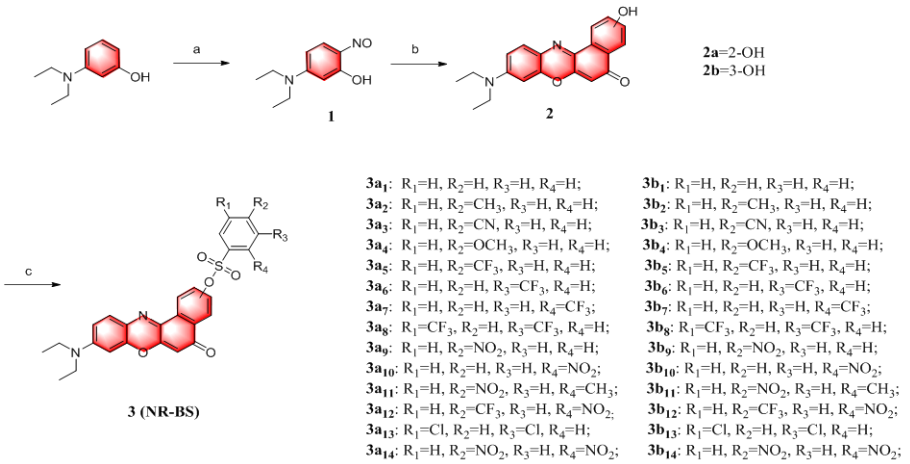

Scheme 1. Synthesis of probes **NR-BS**. (a) $NaNO_2$, HCl, H_2O, 3.5 h, 77.1%; (b) Dihydroxynaphthalene, DMF, reflux, 6 h, 31.3%; (c) Et_3N, DCM, r.t., 2 h.

2.2. Titration experiments of probes **NR-BS**

Before the fluorescence experiment, probes **NR-BS** were prepared as a solution (1.00 mM) by DMF. In addition, Na_2S_2 solution was prepared by reacting $Na_2S{\cdot}9H_2O$ with sulfur in an aqueous solution at 70 ℃ for 1.5 h. In general, the reaction of probes **NR-BS** with Na_2S_2 was performed in PBS (10.0 mM, pH 7.40, 20% DMSO, 100 μM

CTAB). Then, the reaction solution was measured for its fluorescence intensity and scanned at 590 nm.

2.3. Cell imaging

For exogenous imaging, HepG2 cells with **NR-BS4** (5.00 μM) were incubated at 37 ℃ for 30 min, then bred with changed volume of Na_2S_2 (0 μM, 25 μM, 100 μM and 180 μM) for 15 min. For endogenous imaging, HepG2 cells were split into two plates. One disc was stimulated with lipopolysaccharide (LPS, 1.00 $\mu g \cdot mL^{-1}$) for 20 h, and then conducted to incubate with **NR-BS4** for 30 min. The other disc was proceeded to incubate with DL-propargylglycine (PAG, 100 μM) and **NR-BS4** for 30 min, and then LPS was incubate for 20 h. Next, an excitation wavelength of 552 nm was selected to collect the emission light within the limits of 560 to 700 nm, the images were obtained under a confocal laser microscope.

2.4. Zebrafish imaging

Three-day-old zebrafish were selected for imaging and divided into two groups of six fish each. Two groups of fish were loaded with **NR-BS4** and cultured at 28 ℃ for 30 min. One group was performed to incubate with 350 μM Na_2S_2 for 15 min, while the other group was added by E3 medium as a control. Imaging was performed under the same conditions as for cell imaging.

3. Results and discussion

3.1. Design of probes **NR-BS**

Nile red dye (NR) has been recognized as a potential candidate with a wide range of applications due to excellent characteristics, including controllable emission and high photostability. Above all, it has a long fluorescence emission wavelength (λ_{em} > 650 nm), which can effectively reduce the background fluorescence in complex samples, and improve the detection sensitivity and accuracy. As we know, 2, 4-dinitrobenzenesulfonyl is a powerful recognition group for biothiols via nucleophilic substitution [29]. Inspired by this recognition group (Fig. **2a**) and considering the strong nucleophilic properties of H_2S_n, we speculated that this kind of benzenesulfonyl analog should also be able to capture H_2S_n, thereby releasing the

masked fluorophore and restoring its fluorescence. We assumed that the specific detection of H_2S_n could be achieved by changing types and positions of the substituents on the benzene ring of benzenesulfonyl to affect biothiols. Furthermore, it has been found that the different hydroxyl positions of NR will lead to differences in its reactivity and fluorescence properties. To verify the assumptions, we selected 2- or 3- hydroxy NR as the fluorophore scaffold, modified with 14 commercial benzenesulfonyl derivatives, and constructed a series of fluorescent probes **NR-BS**. We presume that the electron-withdrawing groups (-NO_2, -CF_3, -CN, -Cl and -OCH_3) could suppress the fluorescence of NR-OH by way of PET, while the electron-donating group (-CH_3) cannot produce PET process, as a control. When the strongly nucleophilic H_2S_n is added, the sulfonate ester is cleaved, releasing NR-OH with high fluorescence intensity (Fig. **2b**).

The synthesis process is illustrated in **Scheme 1**. Specific synthesis steps and detailed spectra of structural characterization are shown in the Supporting Information.

3.2. Fluorescent spectral properties and responses for H_2S_n

The source of H_2S_2, the main representative compound of H_2S_n, is usually obtained by preparing a fresh Na_2S_2 solution [30]. Within **NR-BS** hand, we firstly tested the spectral properties and responses for Na_2S_2 under imitated physiological circumstances (10.0 mM PBS, pH 7.40, encompassing 20% DMSO and 100 μM CTAB), in which benzenesulfonyl analogs substituted with -NO_2 and -CF_3 produced red fluorescence, named **NR-BS1**, **NR-BS2**, **NR-BS3**, **NR-BS4** and **NR-BS5**, respectively. The response time, linear range, and fluorescence enhancement multiples, were further studied for these five compounds. The fluorescence intensity of **NR-BS1**, **NR-BS2**, **NR-BS3**, **NR-BS4** and **NR-BS5** showed linear relationship within the scope of 0~300 μM, 0~5.00 μM, 0~200 μM, 0~350 μM, and 0~10.0 μM, respectively (Fig. **3**). The selectivity of the five probes for the determination of Na_2S_2 was further compared, and their responses to the interfering molecular biothiols were investigated, and the data are shown in Table **S4**. Considering that **NR-BS4** has the advantages of wide linear range, high response fold, and no interference from biological thiols

compared to the other four compounds, it was selected as a representative probe for follow-up examination.

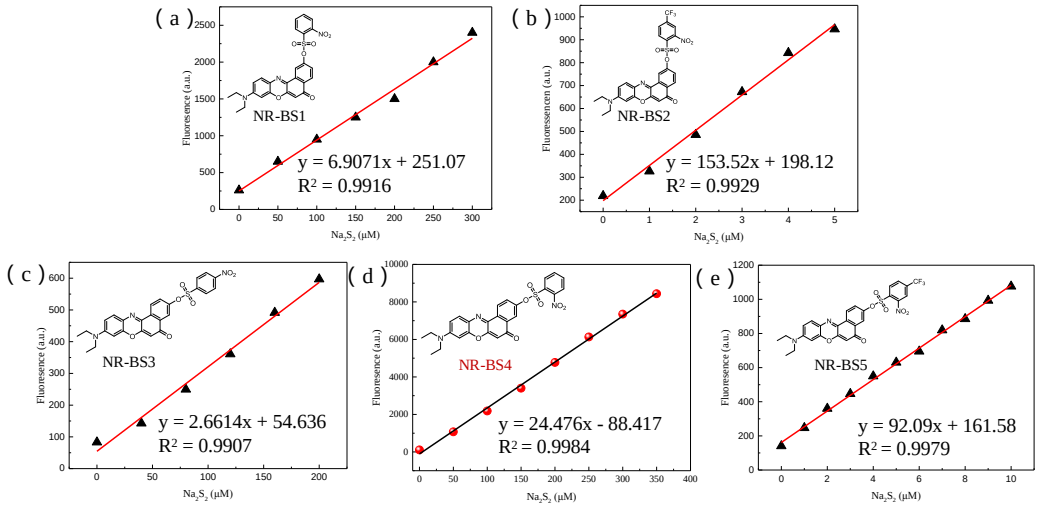

Fig. 3. Linear relationship between probes and Na_2S_2 concentration at 590 nm. (a) 10.0 μM of **NR-BS1** with Na_2S_2 (0~300 μM), (b) 10.0 μM of **NR-BS2** with Na_2S_2 (0~5.00 μM), (c) 10.0 μM of **NR-BS3** with Na_2S_2 (0~200 μM), (d) 10.0 μM of **NR-BS4** with Na_2S_2 (0~350 μM), (e) 10.0 μM of **NR-BS5** with Na_2S_2 (0~10.0 μM).

When **NR-BS4** existed alone, it emitted powerless fluorescence. As Na_2S_2 was gradually added, the fluorescence intensity at 666 nm also gradually enhanced (Fig. **4a**), and the linear range was 0~350 μM (Fig. **4b**, R^2 = 0.9984). According to the formula listed in Table **S2**, LOD was figured up 0.14 μM. These data confirm that **NR-BS4** can achieve quantitative detection of Na_2S_2 in vitro with good selectivity, excellent sensitivity, and wider linear range compared to the published probes listed in Table **S1**.

3.3. Kinetic study of probe **NR-BS4** on H_2S_n

For the purpose of successfully working for biofluorescence imaging, **NR-BS4** must be activated in the proper physiologic pH range. Therefore, we tested the sensitivity of **NR-BS4** to Na_2S_2 at different pH values (2~13) using fluorescence spectrometry (Fig. **4c**). Additionally, the time-driven phenomenon of **NR-BS4** was observed. The fluorescence intensity of **NR-BS4** gradually heightened and reached a plateau at 666 nm for 10 min, and then remained basically unchanged (Fig. **4d**), which proved that **NR-BS4** could be used as a tool to achieve monitoring *in vivo*.

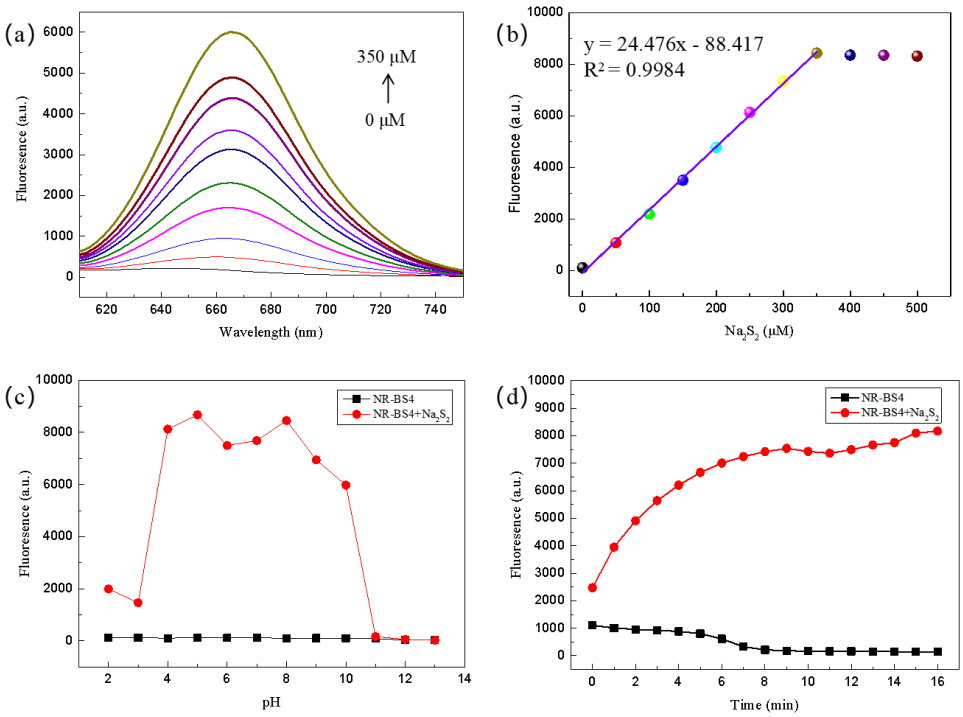

Fig. 4. Spectral properties of probe **NR-BS4**. (a) Fluorescence titration spectrum of probe **NR-BS4** (10.0 μM) with different concentrations of Na_2S_2 (0~500 μM) in PBS (10.0 mM, pH 7.40, 20% DMSO) at room temperature. (b) Linear relationship between probe **NR-BS4** (10.0 μM) at 590 nm and Na_2S_2 concentration (0~350 μM). (c) pH-dependent fluorescence changes of **NR-BS4** (10.0 μM) in the absence and present of Na_2S_2 (350 μM). (d) Time-dependent fluorescence changes of **NR-BS4** (10.0 μM) with Na_2S_2 (350 μM) in phosphate buffer. λ_{ex} = 590 nm, λ_{em} = 666 nm, slits: 5.00 nm / 10.0 nm, volt: 850 V.

3.4. Selectivity and competition of **NR-BS4** to H_2S_n

To determine the selectivity of **NR-BS4** toward Na_2S_2, a series of other fluorescence experiments with interfering small molecules were performed. As shown in Fig. **5a**, the probe **NR-BS4** had only a fluorescence-on response to Na_2S_2. While Na_2S and NaHS caused weak fluorescence enhancement, but it could be ignored. These data demonstrate that **NR-BS4** exhibits good selectivity for Na_2S_2 under physiological conditions. Then the competition of **NR-BS4** in the complex system was measured. Even when other interfering substances were added, the fluorescence signal of **NR-BS4** for Na_2S_2 still existed (Fig. **5b**). These results conclude that **NR-BS4** could selectively respond to Na_2S_2 against a variety of potential interfering species in the biological media.

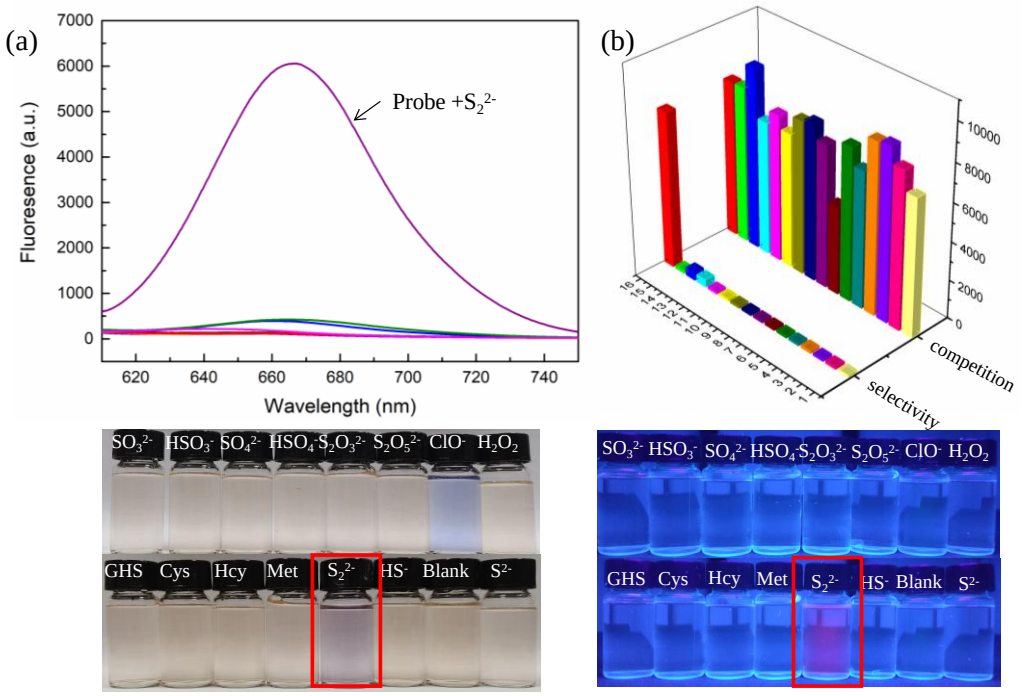

Fig. 5. (a) Fluorescence spectrum of probe **NR-BS4** (10.0 μM) upon addition 350 μM 16 kinds of analytes in PBS buffer solution. (b) Fluorescence spectrum of probe **NR-BS4** (10.0 μM) under simultaneously presence of 350 μM Na_2S_2 and other analytes in PBS buffer solution (1. Na_2SO_3, 2. $NaHSO_3$, 3. Na_2SO_4, 4. $NaHSO_4$, 5. $Na_2S_2O_3$, 6. $Na_2S_2O_5$, 7. NaClO, 8. H_2O_2, 9. GSH, 10. Cys, 11. Hcy, 12. Met, 13. Na_2S, 14. NaHS, 15. Blank, 16. Na_2S_2).

3.5. DFT calculations

In order to fully understand the fluorescence change mechanism of probe **NR-BS4** and compound **2b**, DFT calculations were performed using the B3LYP/6-311+G(d) level of the Gaussian 09 program. The solvent effects were considered in DMF using the polarizable continuum model (PCM). As shown in Fig. **6**, the LUMO energy (-3.68 eV) of 2-nitrobenzenesulfonyl chloride (**DNS**) is between the HOMO energy (-5.18 eV) and LUMO energy (-3.13 eV) of compound **2b**, which proves that PET can happen.

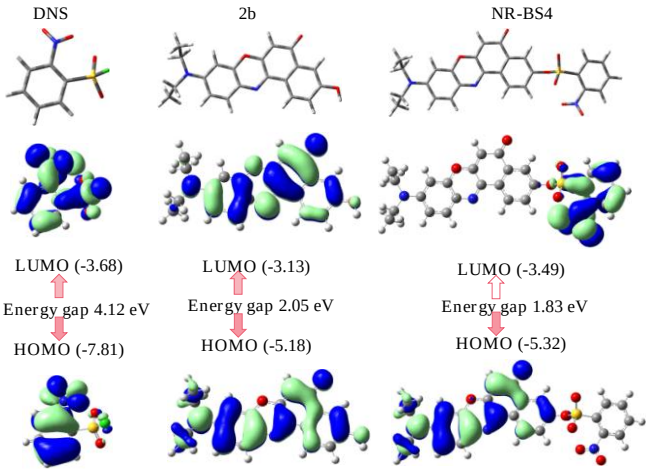

Fig. 6. Structural optimization of **DNB**, compound **2b**, and **NR-BS4** by DFT.

3.6. Reaction mechanism study

The selective response mechanism of probe **NR-BS4** to Na_2S_2 was further studied by LC-MS. As shown in Fig. **7a**, the peak time of free **NR-BS4** in methanol showed 22.5 min. After the addition of Na_2S_2, the signal at 22.5 min decreased, but a new peak appeared at 16 min, $[M+H]^+$ = 335.1353 was determined, which corresponds to the production of compound **2b** (Fig. **7b-c**).

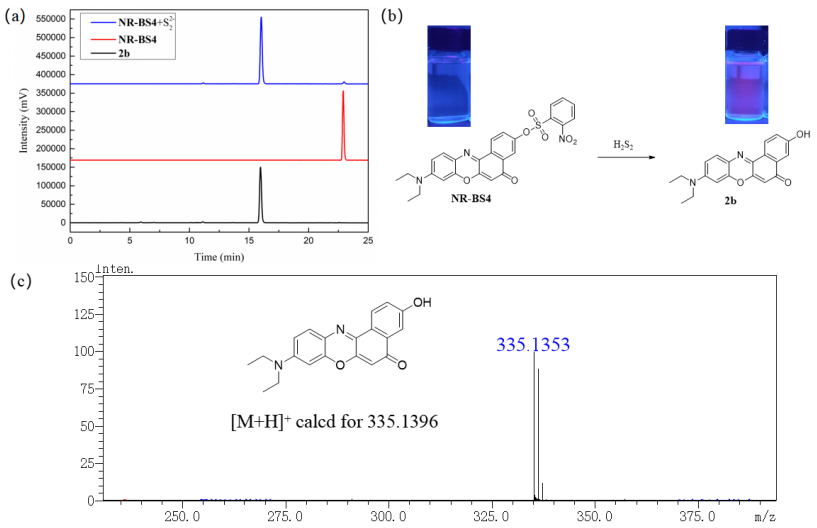

Fig. 7. Reaction mechanism of probe **NR-BS4** with Na_2S_2. (a) LC-MS chromatograms: eluent, CH_3CN/H_2O (gradient elution: 0~5 min, 50/50; 5~10 min, 60/40; 10~15 min, 70/30; 15~20 min, 80/20; 20~30 min, 100% CH_3CN); flow rate, 0.5 mL·min^{-1}; temperature, 30°C; detection wavelength, 542 nm; and injection volume, 10.0 μL; (b) The reaction mechanism of **NR-BS4** towards H_2S_2; (c) HRMS spectrum of the probe **NR-BS4** reacted with H_2S_2.

3.7. Fluorescence imaging in living cells

The cytotoxicity of **NR-BS4** was quantified by the MTT assay prior to biological applications. Fig. **S1** indicates that **NR-BS4** has cytotoxicity, and a concentration of 5.00 μM was selected for subsequent cell imaging.

First, the imaging ability of **NR-BS4** in cells was explored with exogenous Na_2S_2. The weak red fluorescence appeared after probe-loaded HepG2 cells were incubated at 30 min, confirming the good cell permeability of **NR-BS4** (Fig. **8a-c**). When different concentrations of Na_2S_2 were added and incubated for 15 min, followed by 30 min incubation with probe **NR-BS4**, strong red fluorescence was observed (Fig. **8d–i**).

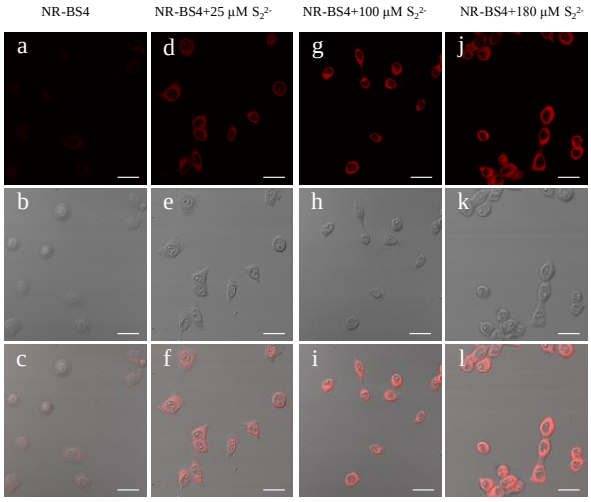

Fig. 8. Confocal fluorescence images of exogenous H_2S_2 in HepG2 cells. HepG2 cell incubated by probe **NR-BS4** (5.00 μM) and observed under red channel (a), bright field (b), overlay (c), then further incubation with Na_2S_2 (25.0 μM, 100 μM and 180 μM) for 15 min and observed under red channel, bright field, overlay.

Furthermore, the imaging capacity of **NR-BS4** to monitor endogenous H_2S_n was also investigated. It has been reported that lipopolysaccharide (LPS) can increase H_2S_n production by inducing CSE mRNA overexpression. Obviously, a dramatical enhancement in intracellular fluorescence intensity can be discovered from Fig. **9a-c**, compared to that of Fig. **8a**. In addition, when DL-propargylglycine (PAG, a CSE inhibitor) was added, the fluorescence intensity was suppressed. These results are consistent with those reported in the literature that CSE contributes to generate endogenous H_2S_n. In conclusion, **NR-BS4** enables the detection of endogenous H_2S_n levels in living cells.

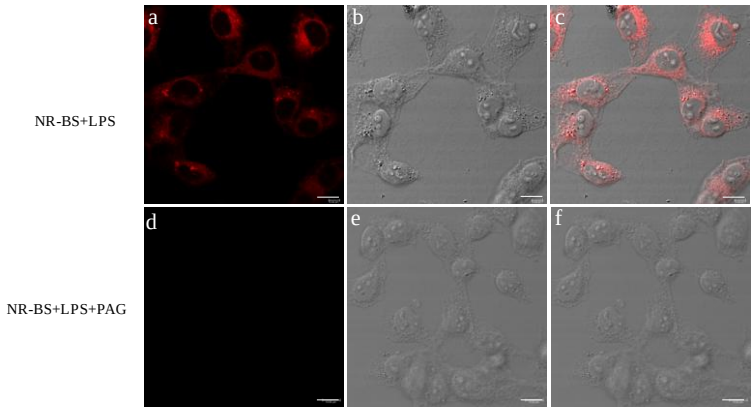

Fig. 9. Fluorescence images of endogenous H_2S_2 in HepG2 cells. HepG2 cell were induced by LPS (1.00 μg/mL) for 20 h, then incubated with 5.00 μM **NR-BS4** for 30 min, and observed under red channel (a), bright field (b), overlay (c); (d) pretreated with DL-propargylglycine (1.00 mM) for 30 min and then treated as (a).

3.8. Fluorescence imaging of H_2S_n in zebrafish

In view of the satisfactory performance of **NR-BS4** in detecting H_2S_n in cells, the applicability of the probe **NR-BS4** in live zebrafish is chosen to be evaluated. As shown in Fig. **10a**, samples loaded with probe **NR-BS4** display medium fluorescence brightness, which was caused by H_2S_n in zebrafish. Probe-loaded zebrafish embryos served with external Na_2S_2 displayed increased fluorescence (Fig. **10b**). These results further demonstrate the promise of probe **NR-BS4** for in vivo imaging.

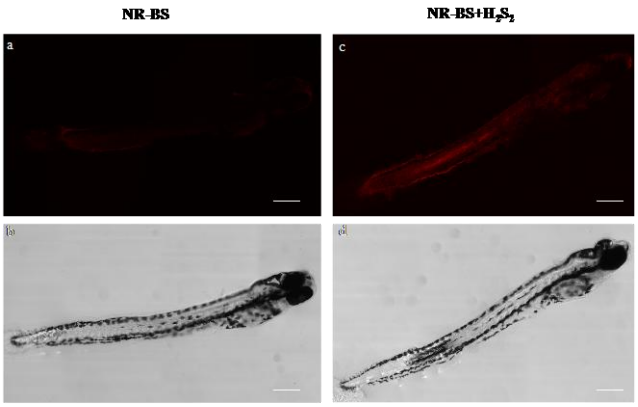

Fig. 10. Fluorescence images of H_2S_2 in zebrafish. 5.00 μM of **NR-BS4** under red channel (a), bright field (b); (c) 5.00 μM of **NR-BS4** incubated with 350 μM of Na_2S_2 for 30 min under red channel, bright field (d).

4. Conclusion

In summary, inspired by the recognition group 2,4-dinitrobenzenesulfonyl of biothiols, we explored the effects of the types and positions of substituent on the benzene ring of benzenesulfonyl on the responses of biothiols and H_2S_n. Furthermore,

we think that the different positions of the hydroxyl groups of NR could lead to differences in its reactivity and fluorescence properties. Based on this, we selected 2- or 3-hydroxy NR as the fluorophore scaffold, modified with 14 commercial benzenesulfonyl derivatives, and constructed a series of fluorescent probes **NR-BS**. After the evaluation of fluorescence properties, the optimal probe **NR-BS4** was found to have a rapid response (< 10 min), high sensitivity (0.140 μM), wide linear range (0~350 μM), large pH tolerance range (pH = 4~10) and good biocompatibility, so as to detect H_2S_n levels in the organism. We believe that our work could provide a new identification group that will be further used to explore the biological and pathological functions of H_2S_n.

Acknowledgements

The authors thank the National Natural Science Foundation of China (No. 21572177), the Key Research and Development Program of Shaanxi Province (No. 2023-YBSF-396), Biomedicine Key Laboratory of Shaanxi Province (No. 2018SZS41).

References

[1] S. Kasamatsu, H. Ihara, Regulation of redox signaling by reactive sulfur species, J. Clin. Biochem. Nutr. 68 (2021) 111-115. https://doi.org/10.3164/jcbn.20-124.

[2] Q. Wang, Z. Chen, X. Zhang, Y. Xin, Y. Xia, L. Xun, H. Liu, Rhodanese Rdl2 produces reactive sulfur species to protect mitochondria from reactive oxygen species, Free Radical Bio. Med. 177 (2021) 287-298. https://doi.org/10.1016/j.freeradbiomed.2021.11.005.

[3] S. Ishii, T. Ashino, H. Fujimori, S. Numazawa, Reactive sulfur species inhibit the migration of PDGF-treated vascular smooth muscle cells by blocking the reactive oxygen species-regulated Akt signaling pathway, Free Radical Res. 55 (2021) 186-197. https://doi.org/10.1080/10715762.2021.1887485.

[4] N. Takahashi, F.Y. Wei, S. Watanabe, M. Hirayama, Y. Ohuchi, A. Fujimura, T. Kaitsuka, I. Ishii, T. Sawa, H. Nakayama, T. Akaike, K. Tomizawa, Reactive sulfur species regulate tRNA methylthiolation and contribute to insulin secretion, Nucleic Acids Res. 45 (2017) 435-445. https://doi.org/10.1093/nar/gkw745.

[5] H.J. Sun, Z.Y. Wu, X.W. Nie, J.S. Bian, Role of hydrogen sulfide and polysulfides in neurological diseases: focus on protein S-persulfidation, Curr. Neuropharmacol. 19 (2021) 868-884. https://doi.org/10.2174/1570159X18666200905143550.

[6] S. Yamanaka, T. Ichikawa, H. Sugiura, T. Numakura, H. Sano, M. Yamada, N. Fujino, R. Tanaka, Y. Kyogoku, T. Akaike, M. Ichinose, Reactive sulfur species are involved in cigarette

smoke-induced cellular senescence, Eur. Respir. J. 54 (2019) 1-5. 10.1183/13993003.congress-2019.PA4055.

[7] X. Cao, W. Zhang, P.K. Moore, J. Bian, Protective smell of hydrogen sulfide and polysulfide in cisplatin-induced nephrotoxicity, Int. J. Mol. Sci. 20 (2019) 1-15. https://doi.org/10.3390/ijms20020313.

[8] Q. Zhang, Z. Shen, Y. Shen, M. Ma, H. Jue, Y. Zhu, W. Guo, The regulatory role of MiR-203 in oxidative stress induced cell injury through the CBS/H_2S pathway, Nitric Oxide-Bio. Ch. 118 (2022) 31-38. https://doi.org/10.1016/j.niox.2021.10.007.

[9] H.T. Liu, Z.X. Zhou, Z. Ren, S. Yang, L.S. Liu, Z. Wang, D.H. Wei, X.F. Ma, Y. Ma, Z.S. Jiang, Potential target of H_2S against atherosclerosis, Curr. Med. Chem. 28 (2021) 3666-3680. https://doi.org/10.2174/0929867327999201116194634.

[10] T.Z. Liu, X.L. Cui, W.L. Sun, J.Y. Miao, B.X. Zhao, Z.M. Lin, Two simple but effective turn-on benzothiazole-based fluorescent probes for detecting hydrogen sulfide in real water samples and HeLa cells, Anal. Chim. Acta 1189 (2022) 339225-339234. https://doi.org/10.1016/j.aca.2021.339225.

[11] K. Zhong, Y.Q. He, L.L. Deng, X.M. Yan, X.P. Li, Y.W. Tang, S.H. Hou, L.J. Tang, A near-infrared fluorescent probe for H_2S based on tandem reaction to construct iminocoumarin-benzothiazole and its application in food, water, living cells, Anal. Chim. Acta 1127 (2020) 49-56. https://doi.org/10.1016/j.aca.2020.06.050.

[12] H. Kimura, Signalling by hydrogen sulfide and polysulfides via protein S-sulfuration, Brit. J. Pharmacol. 177 (2020) 720-733. https://doi.org/10.1111/bph.14579.

[13] H. Kimura, Signaling molecules: hydrogen sulfide (H_2S) and polysulfides (H_2S_n), J. Pharmacol. Sci. 133 (2017) S15-S15. https://doi.org/10.1016/j.freeradbiomed.2016.04.034.

[14] P.K. Yadav, M. Martinov, V. Vitvitsky, J. Seravalli, R. Wedmann, M.R. Filipovic, R. Banerjee, Biosynthesis and reactivity of cysteine persulfides in signaling, J. Am. Chem. Soc. 138 (2016) 289-299. https://doi.org/10.1021/jacs.5b10494.

[15] K.R. Olson, Y. Gao, Effects of inhibiting antioxidant pathways on cellular hydrogen sulfide and polysulfide metabolism, Free Radical Bio. Med. 135 (2019) 1-14. https://doi.org/10.1016/j.freeradbiomed.2019.02.011.

[16] K. Yang, I. Coburger, J.M. Langner, N. Peter, T. Hoshi, R. Schoenherr, S.H. Heinemann, Modulation of K^+ channel N-type inactivation by sulfhydration through hydrogen sulfide and polysulfides, Pflug. Arch. Eur. J. Phy. 471 (2019) 557-571. https://doi.org/10.1007/s00424-018-2233-x.

[17] H.J. Sun, B. Leng, Z.Y. Wu, J.S. Bian, Polysulfide and hydrogen sulfide ameliorate cisplatin-induced nephrotoxicity and renal inflammation through persulfidating STAT3 and IKK beta, Int. J. Mol. Sci. 21 (2020) 7805-7822. https://doi.org/10.3390/ijms21207805.

[18] C. Debiemme-Chouvy, C. Wartelle, F.X. Sauvage, First evidence of the oxidation and regeneration of polysulfides at a GaAs electrode, under anodic conditions. A study by in situ UV-visible spectroelectrochemistry. J. Phys. Chem. B 108 (2004) 18291-18296. https://doi.org/10.1021/jp046977y.

[19] J. Gun, A.D. Modestov, A. Kamyshny, D. Ryzkov, V. Gitis, A. Goifman, O. Lev, V. Hultsch, T. Grischek, E. Worch, Electrospray ionization mass spectrometric analysis of aqueous polysulfide solutions, Microchim. Acta 146 (2004) 229-237. https://doi.org/10.1007/s00604-004-0179-5.

[20] S. Koike, K. Kawamura, Y. Kimura, N. Shibuya, H. Kimura, Y. Ogasawara, Analysis of endogenous H_2S and H_2S_n in mouse brain by high-performance liquid chromatography with fluorescence and tandem mass spectrometric detection, Free Radical Bio. Med. 113 (2017) 355-362. https://doi.org/10.1016/j.freeradbiomed.2017.10.346.

[21] X.Y. Zhao, M.B. Ding, L.L. Ning, F. Yuan, J.C. Li, Y. Guo, Y.G. Mu, J.J. Zhang, Biothiol-triggered H_2S release from a near-infrared fluorescent H_2S donor promotes cutaneous wound healing. Acta Materia Medica. 1(2022)476-485. https://doi.org/10.15212/AMM-2022-0032.

[22] X.L. Li, Q. Feng, L.J. Qu, T. Zhao, X.A. Li, T.T. Bai, S.S. Sun, S.P. Wu, Y.M. Zhang, J.L. Li, A water-soluble and incubate-free fluorescent environment-sensitive probe for ultrafast visualization of protein thiols within living cells, Anal. Chim. Acta 1126 (2020) 72-81. https://doi.org/10.1016/j.aca.2020.06.026.

[23] C. Liu, W. Chen, W. Shi, B. Peng, Y. Zhao, H. Ma, M. Xian, Rational design and bioimaging applications of highly selective fluorescence probes for hydrogen polysulfides, J. Am. Chem. Soc. 136 (2014) 7257-7261. https://doi.org/10.1021/ja502968x.

[24] J. Sun, Y. Bai, Q. Ma, H. Zhang, M. Wu, C. Wang, M. Tian, A FRET-based ratiometric fluorescent probe for highly selective detection of hydrogen polysulfides based on a coumarin-rhodol derivative, Spectrochim. Acta A 241 (2020) 118650-118658. https://doi.org/10.1016/j.saa.2020.118650.

[25] W. Chen, E.W. Rosser, D. Zhang, W. Shi, Y. Li, W.J. Dong, H. Ma, D. Hu, M. Xian, A specific nucleophilic ring-opening reaction of aziridines as a unique platform for the construction of hydrogen polysulfides sensors, Org. Lett. 17 (2015) 2776-2780. https://doi.org/10.1021/acs.orglett.5b01194.

[26] J. Chung, H. Li, C.S. Lim, H.M. Kim, J. Yoon, Two-photon imaging of hydrogen polysulfides in living cells and hippocampal tissues, Sensor. Actuat. B-Chem. 322 (2020) 128564-128571. https://doi.org/10.1016/j.snb.2020.128564.

[27] Y. Hou, X.F. Yang, Y. Zhong, Z. Li, Development of fluorescent probes for hydrogen polysulfides by using cinnamate ester as the recognition unit, Sensor. Actuat. B-Chem. 232 (2016) 531-537. https://doi.org/10.1016/j.snb.2016.04.008.

[28] J. Guo, S. Yang, C. Guo, Q. Zeng, Z. Qing, Z. Cao, J. Li, R. Yang, Molecular engineering of alpha-substituted acrylate ester template for efficient fluorescence probe of hydrogen polysulfides, Anal. Chem. 90 (2018) 881-887. https://doi.org/10.1021/acs.analchem.7b03755.

[29] W. Zhang, C. Yin, Y. Zhang, J. Chao, F. Huo, A turn-on fluorescent probe based on 2, 4-dinitrosulfonyl functional group and its application for bioimaging, Sensor. Actuat. B-Chem. 233 (2016) 307-313. https://doi.org/10.1016/j.snb.2016.04.089.

[30] M. Gao, R. Wang, F. Yu, J. You, L. Chen, A near-infrared fluorescent probe for the detection of hydrogen polysulfides biosynthetic pathways in living cells and in vivo, Analyst 140 (2015) 3766-3772. https://doi.org/10.1039/C4AN02366H.